THE AMERICAN SOCIETY OF MECHANICAL ENGINEERS
345 E. 47th St., New York, N.Y. 10017

98-GT-585

THERMODYNAMIC ANALYSIS OF ADVANCED POWER CYCLES BASED UPON SOLID OXIDE FUEL CELLS, GAS TURBINES AND RANKINE BOTTOMING CYCLES

S. Campanari
PhD Candidate
Energetics Dept., Politecnico di Milano
E-Mail: scampanari@clausius.energ.polimi.it

E. Macchi
Full Professor of Energy Conversion
Energetics Dept., Politecnico di Milano
Piazza Leonardo da Vinci 32, 20133 Milan - Italy
E-Mail: profmacc@clausius.energ.polimi.it

Abstract

This paper investigates the thermodynamic potential of the integrated Solid Oxide Fuel Cell – Gas Turbine technology for medium and large scale electric power production. After detailed description of the adopted calculation model, the performances of a variety of plant configurations are presented. The obtained results show the possibility of achieving very high efficiencies with pressurized SOFC-gas turbine cycles with heat recovery bottoming cycles: net LHV efficiencies exceeding 70% with almost zero-NO_x emissions.

Nomenclature

E	reversible cell potential (V)
F	Faraday's constant (96439 Coulomb/mol of electrons) (eq.1)
i	cell current density (mA/cm^2)
m	mass flow (kg/s)
n	number of electrons involved by a reaction (eq.1)
N_S	specific speed: $N_S=RPS*\Gamma^{1/2}/\Delta h_{is}^{3/4}$
p	pressure (Pa)
P_{el}	electric power (MW)
Q_{th}	thermal power (MW)
SP	size parameter: $SP=\Gamma^{1/2}/\Delta h_{is}^{1/4}$ (m)
T	temperature (°C or K)
U_a	air utilization factor: $U_a=O_{2,consumed} / O_{2,inlet}$
U_f	fuel utilization factor: $U_f=(H_{2,consumed})/(H_{2,in}+CO_{in}+4CH_{4,in})$
V_c	cell voltage (V)
W_{el}	electric work (kJ/kg)
W_{rev}	reversible work (kJ/kg)
β	pressure ratio
$\Delta\eta_{II}$	2nd law efficiency loss
ΔG	Gibbs free energy variation (J/mol)
Δh_{is}	isentropic enthalpy change in a turbomachinery stage (kJ/kg)
ΔS	entropy variation (kJ/(kg*K))
η_p	polytropic efficiency
η_{el}	electric efficiency (eq.2)
η_{th}	thermal efficiency
Γ	volume flow rate (outlet for turbine stage, average for compressor stages, m^3/s)

Subscripts

a	air
amb	ambient
c	cell
el	electric
f	fuel
th	thermal
comb	combustion or oxidization process

Acronyms

AD	aero-derivative
BC	bottoming cycle
DC/AC	direct / alternate current
EFCC	externally fired combined cycle
FC	fuel cell
GT	gas turbine
HD	heavy-duty
HRSG	heat recovery steam generator
HRVG	heat recovery vapor generator
IGCC	Integrated gasification-combined cycle
LHV	lower heating value (kJ/kg)
NGCC	natural gas combined cycle
RH	reheat
RPM	revolutions per minute
RPS	revolutions per second
SH	superheat
SOFC	solid oxide fuel cell
ST	steam turbine
STCR	steam-to-carbon ratio
TIT	turbine inlet temperature
VR	outlet/inlet volume ratio across a turbine stage

Presented at the International Gas Turbine & Aeroengine Congress & Exhibition

1. INTRODUCTION

It is well known that the most relevant irreversibilities in modern, high efficiency combined cycles take place in the combustion process. Even at the very high temperatures nowadays adopted in advanced gas turbines, almost 30% of the fuel potential mechanical work is wasted during the combustion process. This loss can be reduced only by increasing combustion temperatures. However, the impressive rate of increase of maximum hot gas temperature achieved by the gas turbine industry during the past decades (about 15°C/year; Chiesa et al.,1993) will not last forever, due to the tremendous advancement required in cooling and material technology and NOx control. Fuel-cell technology is the most promising long-term answer to overcome these difficulties and achieve substantial improvements of conversion efficiency.

This paper investigates the thermodynamic potential of solid-oxide fuel cells, when integrated with proper power cycles. The first section of the paper addresses the analytical model adopted for predicting the fuel cell performance at various operating conditions (pressure, temperature, air-fuel ratio etc.): reference is made to the tubular technology developed by Westinghouse, with natural gas feeding, internal reforming and working temperatures in the range of 1000°C (Bessette and George,1996 , Veyo,1996a), and to methodology and assumptions adopted for predicting the performance of other more conventional plant components (turbomachines, heat exchangers, etc.).

Subsequently, a number of representative power cycle configurations are investigated, whereby fuel is introduced either in the fuel cell process only or both in the fuel cell and in a subsequent combustor. Simple, regenerative as well as inter-cooled gas cycles are considered: hot exhaust gases exiting the fuel cell are expanded by the gas turbine and finally exploited by a heat recovery bottoming cycle, either a multi-pressure steam cycle or an ammonia supercritical cycle. Calculations are performed based on state-of-the art performance of turbomachinery fluid-dynamic and cooling techniques, with reference to large-scale industrial gas turbines as well as to aero-derivative medium-scale machines. Detailed results are presented, in terms of energy and mass balances and second-law analysis.

2. CALCULATION MODEL

The thermodynamic model of gas-turbine based power cycles is made with a simulation code described by Chiesa et al. (1993), Consonni et al. (1991), Consonni (1992), Lozza (1990 and 1993). In its original version, the modular structure of this computer code allows the analysis of any power cycle described by a network of components chosen among 11 types (pump, compressor, combustor, turbine, mixer, heat exchanger, splitter, heat recovery steam cycle, oxygen plant, shaft+electrical generator, saturator, chemical converter). Among other distinctive characteristics of the code, we remind that the polytropic efficiency of the turbomachines is internally evaluated as a function of the aerodynamic load and the volumetric flow and that the calculation provides a detailed evaluation of the gas turbine blades cooling flows, drawn at decreasing pressure from the compressor. Figure 1 shows the polytropic efficiency calculated by the model for aero-derivative and heavy duty compressors/gas turbines and for steam or ammonia turbines as a function of the size parameter SP (Macchi and Perdichizzi,1981); the curves are traced at optimized specific speed with the exception of the steam turbine curve, for which it is assumed a single-shaft configuration at 3000 rpm

The calculation of energy and mass-balances is repeated sequentially for the various components until convergence is reached, with the eventual optimization of some user-defined variables; the final solution is provided with all the exergy and reversible work fluxes characterizing the plant nodes.

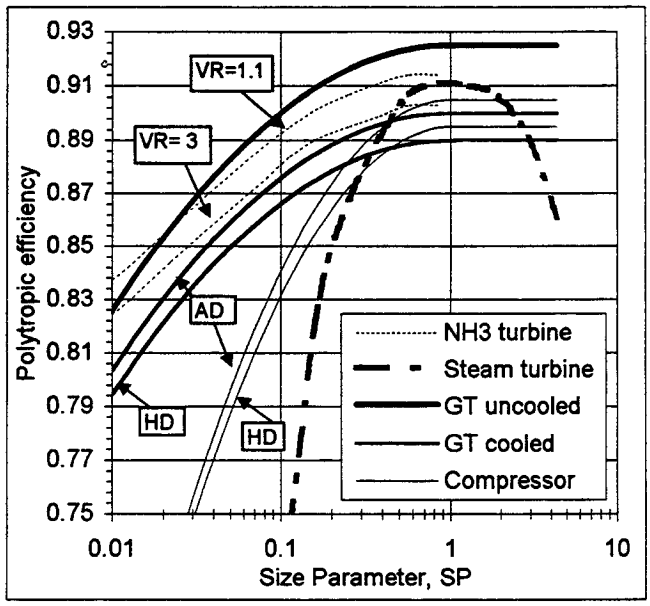

Fig.1: Optimized efficiency η_p predicted by the calculation model for gas, steam and ammonia turbines and compressors.

The simulation code, that proved to yield highly accurate results in a variety of complex plant configurations, including all kind of gas turbine cycles (Consonni et al.,1991 , Macchi et al.,1994), IGCC (Lozza et al.,1996) , EFCC (Consonni and Macchi, 1996), etc., was modified to implement the new element "fuel cell" (Campanari and Macchi, 1997).

2.1 Introduction to the FC Model

Among the different fuel cell (FC) technologies actually under development, we consider here the high-temperature fuel cells, characterized by the interesting possibility of being employed in conjunction with thermodynamic cycles based upon turbomachinery, reaching very high plant electric efficiencies. Solid Oxide Fuel Cells (SOFC) in particular should achieve some advantages in terms of life durability and ease in pressurized operation with respect to other technologies (Penner et al.,1995).

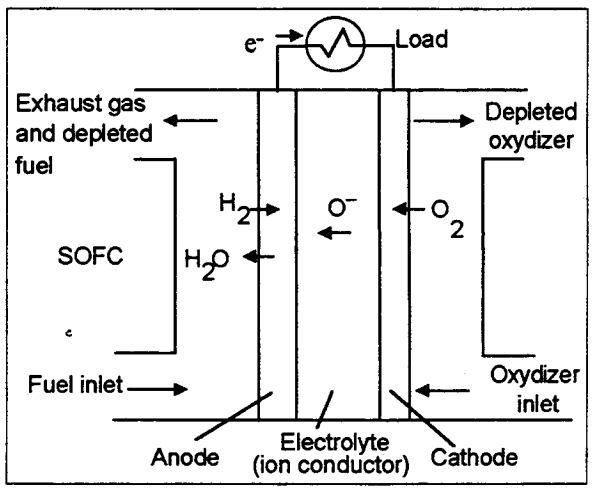

Fig.2: Basic SOFC operating principles.

The SOFC operating principles are described in fig.2: the FC is fed by an oxidizer (air or pure oxygen) and a fuel, which is in general a purified mixture of CH_4 - H_2 - CO - CO_2 - H_2O and inerts (N_2) resulting from the reforming of either desulphurized natural gas or syngas[1]. The two fluxes flow in contact with cathode and anode porous surfaces, separated by a solid electrolyte which is a good $O^=$ ion-conductor at the high SOFC operating temperatures. The reduction of molecular oxygen to $O^=$ takes place at the cathode while hydrogen is oxydized to steam at the anode.

The combustion process is thus substituted by a progressive oxidization. The fuel mixture could contain also carbon monoxide, which can be directly oxidized, and CH_4; as the dominant reaction is anyway the hydrogen oxidization, the CO and CH_4 consumption is modelled by steam reforming and water-gas shift reactions (Achenbach,1994, Appleby, 1995, Kinoshita et al.,1988).

The maximum work of a FC operating at constant temperature and pressure is given by the Gibbs free energy variation for the electrochemical reaction taking place in the cell:

$$W_{el}=\Delta G=-nFE \quad (J/mol) \qquad (1)$$

where n is the number of electrons involved in the reaction; F is the Faraday's constant and E is the reversible cell potential, given by the Nernst equation (Hirschenhofer et al.,1994). The value of E is a function of temperature, ranging in standard conditions for the hydrogen oxidization from 1.229 V at 298 K to 0.909 V at 1273 K. The FC generates direct current electrical energy with an efficiency proportional to its voltage; this voltage is lower than the Nernst potential, due to irreversibilities (over-potentials). Neither all the fuel is oxidized at the anode, nor all the oxygen is consumed at the cathode, to avoid large voltage losses due to reactant concentration gradients and limited gas diffusivity near the active electrodes area; air and fuel utilization factors (see nomenclature) are adopted to quantify these effects. The SOFC electric efficiency is conventionally defined as:

$$\eta_{el}=\frac{W_{el}}{LHV}. \qquad (2)$$

Planar, monolithic and tubular solid oxide fuel cells are currently being developed (Ahmed et al.,1991, Hsu et al.,1994). Even if the former technologies seem to promise best performance at probably lower costs, they are presently at a much earlier development step than the tubular technology (Hirschenhofer, 1996, Appleby,1994, Appelby and Foulkes,1989). We make here reference to the latest generation of the tubular SOFC, the Westinghouse Air Electrode Supported (AES) fuel cells, with operating temperature of 1000°C.

2.2 FC model and performance

The SOFC schematic is shown in fig.3. The fuel is desulphurized natural gas, internally reformed by the SOFC itself: this practice allows a plant simplification and an optimal thermodynamic exploitation of the fraction of the heat rejected by the fuel cell, employed to support the endothermal reforming reactions. The SOFC module is provided with a pre-reformer and partial exhaust fuel recirculation (Ray et al.,1992, Veyo,1996a), sustained by fresh-fuel-driven ejectors. By this practice: 1) the steam required for a complete methane steam-reforming is obtained by exhaust recirculation; the steam-to-carbon ratio, defined as the ratio between the number of H_2O molecules and the number of C atoms in the combustible species (Achenbach,1994, Appelby,1995, Mozzafarian,1994) is in the range 2÷2.5; 2) the heavier hydrocarbons (ethane, pentane, butane) are cracked before entering the anode; 3) the global fuel utilization rises from the 85% of a single passage to about 93%.

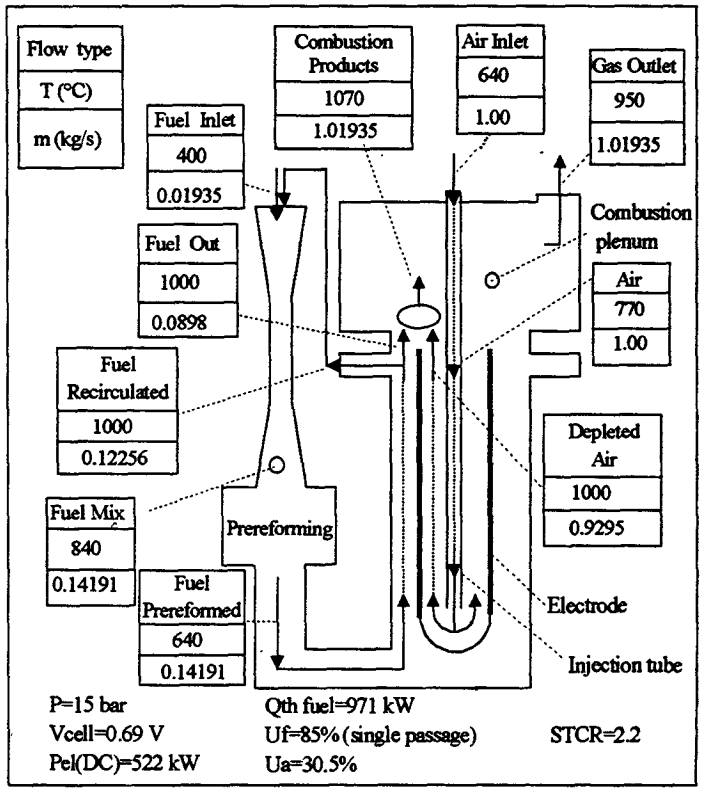

Fig.3: Tubular SOFC module schematic: the anode-electrolyte-cathode structure is tube-shaped, with the air flow inside and the fuel flow outside; spent fuel is partially recirculated.

Mixing and pre-reforming are calculated as adiabatic processes with the simplifying hypothesis of chemical equilibrium. The cell voltage, which is proportional to the cell efficiency, is a function of current density, as shown in fig.4 for reference conditions (Appelby,1995 , Hirschenhofer et al, 1994).

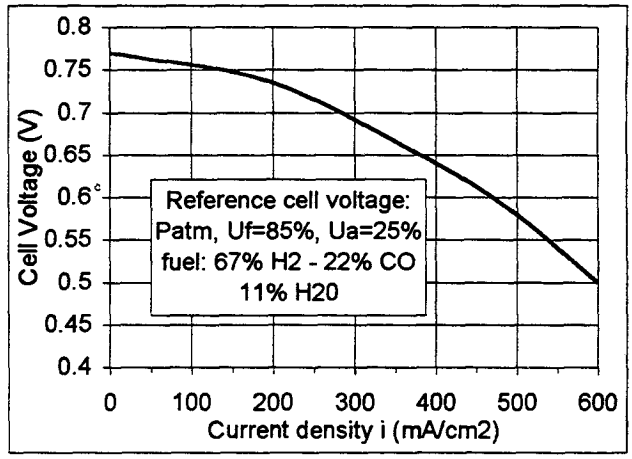

Fig.4: Reference cell voltage.

The cell voltage is also a function of temperature, pressure, current density, fuel and oxidizer composition and utilization factors, and is reduced by impurities and along the cell life. The effects of these variables are accounted by theoretical and experimental

[1] In the present paper reference is made to natural gas as a fuel and air as an oxidizer.

relations given by literature (Hirschenhofer et al.1994, Bessette and George,1996, Hide et al.,1989, Campanari and Macchi, 1997), neglecting only impurities and cell life effects; these correlations make it possible to predict the cell voltage starting from the reference values given by fig.4. The cell voltage hereby predicted shows good agreement with data stated by Westinghouse for operating pressures of 1-30 bar (Veyo,1996b, Bevc et al.,1996), with cell voltage and efficiency rising at increased pressures.

Input data of the calculation model are the following: inlet flow properties (T,p, composition); the oxidizer mass flow; the utilization factors U_f, U_a, and the cell current density i. Output data are: the properties (T,p, composition, mass flow) of inlet, recirculated, mixed and pre-reformed fuel, of preheated and depleted oxidizer, of burned and exhaust flows, as well as energy and mass balances, cell voltage and efficiency.

Differently from SOFC models adopted by other authors (see for example Stephenson and Ritchey, 1997), the SOFC exhaust temperature is not considered as a constant value, but is calculated as a function of the air/fuel inlet temperature, the air/fuel utilization factors and the cell voltage and efficiency.

The temperature of the compressed air fed to the fuel cell module is generally in the range 500÷700°C: with U_a fixed, by increasing or lowering this temperature, the cell exhaust temperature becomes higher or lower after the internal air preheating. It should be noted that the effective air temperature at the cell electrodes inlet is always close to 900°C: small variations can occur to ensure a correct cell cooling, but the temperature must be high enough to allow the solid electrolyte operation.

Preliminary studies show that an increase of the fuel cell air utilization rises the SOFC exhaust temperature, generally increasing the global SOFC+GT cycle efficiency too. We consequently adopted an air utilization factor of about 30%, greater than values of 20÷25% of other studies, in order to investigate the possibility of obtaining best global efficiencies. The resulting SOFC module air inlet temperature are however consistent with those adopted by Westinghouse in recent demonstration plants and with those quoted by EPRI and other research institutes (Ray e Ruby,1992, Lundberg et al.,1996).

Δp/p air/fuel side	5% / 5%
Δp/p fuel at ejectors	50%
Heat loss SOFC	2%
Combustion efficiency	99%
DC-AC efficiency	97%
Fuel inlet temperature	400°C
Fuel utilization factor (single passage)	85%
Air utilization factor	30.5%
Operating temperature	1000°C
Current density	400 mA/cm^2
STCR	2.2
Fuel (natural gas) composition: CH_4 98% - C_2H_6 0.6% - C_3H_8+C_4H_{10} 0.3% - H_2S 0.1% - N_2 1%	
Fuel pressure	45 bar

Tab.1: SOFC model assumptions.

The operating pressure is kept in the range of 1÷30 bar. Fuel cells are generally characterized by a lower power density than conventional engines and turbomachines; with pressurized operation, the FC power density increases, but other problems (large pressurized vessels operating at high temperature) rise. These aspects, linked to detailed plant design (module distribution, thermal insulation) are beyond the scope of this paper.

The main assumptions in the SOFC model are shown in tab.1: the air utilization is about 30% and the current density is 400 mA/cm^2 (with a reference cell voltage of 0.64 V). These values can certainly be adopted in the latest-generation tubular SOFC; as an example EPRI already considered configurations with U_a=15÷33%, i=100÷700 mA/cm^2 (Ray and Ruby,1992), while other authors have assumed U_a=50% (Kaneko et al.,1991).

The FC generates direct current electrical energy (DC), converted into alternate current (AC) by a power conditioner with an efficiency of 97% (Ray and Ruby,1992). Natural gas is preheated at about 400°C to obtain the best efficiency in H_2S adsorption by mean of catalytic Zinc-Oxide beds; the H_2S concentration must be kept under 0.1 ppmv to avoid cell degradation (Ray and Ruby,1992, Lundberg,1990).

2.3 Bottoming Cycles

The hot exhaust gases at atmospheric pressure discharged by the SOFC-gas turbine cycle can be exploited by a heat recovery vapor generator to produce high pressure vapor expanded by a turbine. Two possibilities are examined: (i) an advanced heat recovery steam cycle with 3 levels of evaporating pressure and reheat (Lozza, 1990), and (ii) a super-critical single-level heat recovery cycle using ammonia as working fluid (Campanari et al.,1995).

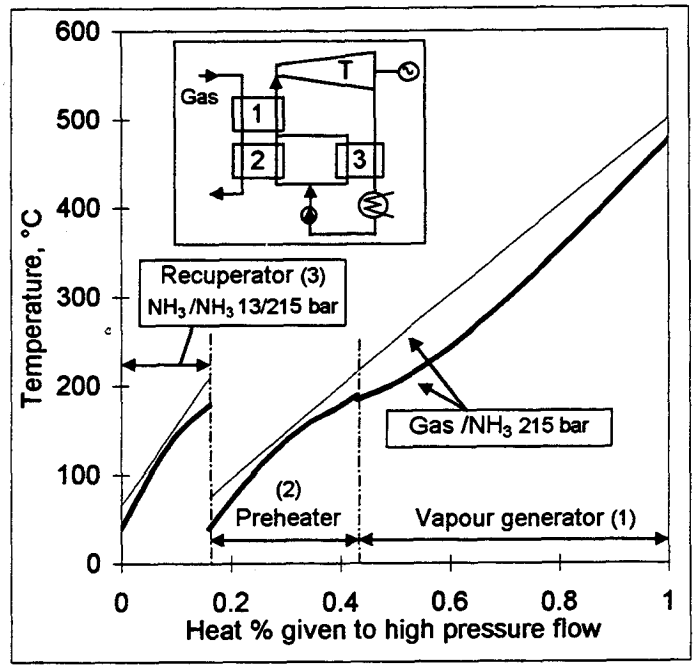

Fig.5: Gas-ammonia temperature profiles.

At low gas temperatures (say, below 400°C) an ammonia cycle, without the complexity of a multi-level cycle, can attain the following advantages:

- optimal gas cooling: exhaust gases exit the once-trough super-critical vapor generator at 55÷75°C;
- gas-working fluid heat-exchange with low temperature differences: mean logarithmic temperature differences are in the range of 20÷30°C, with pinch-point of 10°C;
- the adoption of a compact, single-entry, single-shaft turbine, rotating at high speed (i.e. 8000÷15000 RPM), with a much

lower expansion ratio (i.e. 6÷15 vs 600÷1000) than a steam turbine, lower number of stages (i.e. 6 vs 20) and a better overall isentropic expansion efficiency, less influenced by size effects, high Mach numbers, liquid formation, etc.;

- the possibility of easily exploiting low condensing temperatures: the NH_3 condensation pressure at 24°C is about 10 bar.

At higher gas temperatures (above 400÷450°C) it is possible to recuperate the heat of de-superheating by preheating a fraction (about 40% at optimum design point) of the high-pressure liquid ammonia before entering the heat recovery vapor generator. This configuration is shown in fig. 5 together with typical gas-ammonia temperature profiles. The assumptions related to performance of heat recovery cycle components are given in tab.2.

Heat recovery bottoming cycle
Steam cycle (3 lev.+ rh) thermal losses, auxiliary consumption, pump efficiency, ΔTapproach/pinch/subcooling, Δp/p, max steam SH/RH temperature, LP/deaereator pressure, mec./electric /gear box efficiency: see Lozza,1993; condenser pressure 0.05 bar.
Turbine efficiency: see fig.1.
NH_3 cycle (ipercritical 1 lev.)
Evaporator pressure= 130÷250 bar, Δp/p=6%
Condenser pressure=12.4 bar (32°C), Δp/p=3%
Δp/p desuperheater = 2% ; ΔT gas-NH_3 cold side=15÷40°C
NH_3 Turbine efficiency: see fig.1.

Tab.2: Main assumptions for bottoming cycle calculations.

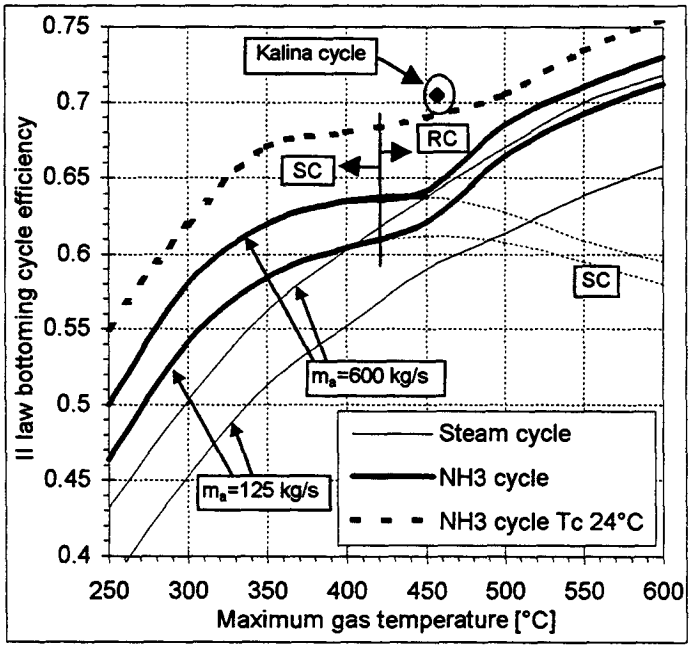

Fig.6: Bottoming cycle performances. RC=recuperated cycle, SC=simple cycle; top curve for NH_3 simple/recuperated cycle with condensation at 24°C.

Figure 6 compares the performance of ammonia and steam cycles in terms of II law efficiency η_{II} (defined as the ratio between the electric work generated and the maximum reversible work of the hot gas flows) at various hot gas temperatures. Results are given for the two mass flows considered in the paper: (i) 600 kg/s, typical of a large heavy-duty "F" gas turbine operating at 50 Hz and (ii) 125 kg/s, typical of large aero-derivative machines. As expected, advantages of ammonia cycles hold only for relatively low gas temperatures, say below 450 °C and/or for very low condensation temperatures. It is interesting to note that the much more complex Kalina Cycle (with three turbines operating at different speed, a number of heat exchangers and a bulky distillation-condensation subsystem with lowest temperature of about 17°C) achieves a global II law efficiency just 2% greater (Lobachyov and Richter, 1997).

3. PLANT CONFIGURATIONS AND THERMODYNAMIC RESULTS

Let's first discuss two relevant points: (i) the potential advantages in terms of combined cycle efficiency achievable by substituting the combustion process taking place in gas turbines by electrochemical reaction and (ii) the importance of exergy fluxes related to flow rates and thermodynamic conditions of fluids entering and leaving the fuel cell.

As far as the first point is concerned, it is well known that the main advantage of the fuel cells is the possibility of accomplishing the direct electrochemical conversion of the fuel chemical energy into electrical energy, thereby skipping the combustion reaction and the heat-to-work conversion. The reversible work losses of a simple combustion process and of a SOFC are compared in fig. 7. These losses are defined as:

$$\Delta\eta_{II} = \frac{T_{amb}\Delta S}{Wrev_f} \quad . \qquad (3)$$

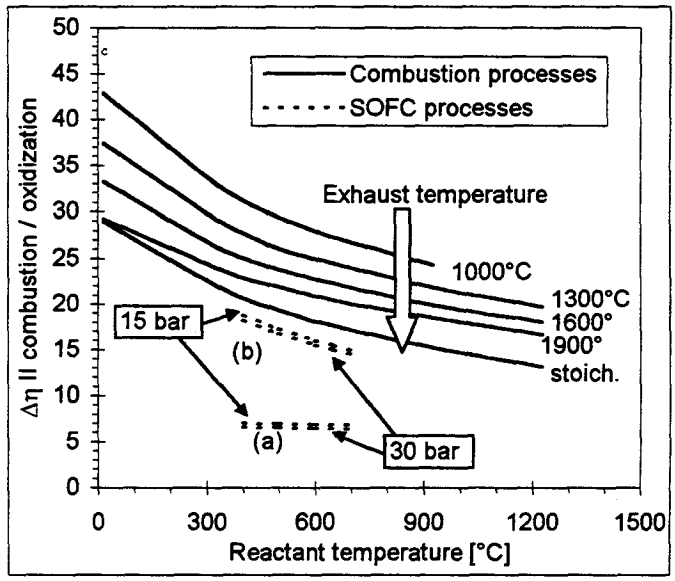

Fig.7: Second law losses for a combustion and a SOFC process.

The figure shows that a simple combustion with reactants at 400°C and products at 1350°C, representative of the combustion process of a modern heavy-duty gas turbine cycle with β=15, contributes a reversible work loss close to about 28%; this loss can be reduced down to 20% only by increasing product temperatures up to 1900÷2000°C and preheating the reactants to at least 750÷800°C, thereby exiting from the technologically acceptable temperatures range. On the contrary, the fuel cell achieves reversible work losses of about 7% considering electrochemical and heat exchange losses only (curves "a" in fig.7), or close to 16% (curves "b" in fig.7), considering also recirculation, mixing, reforming, preheating and exhaust combustion losses.

The potential advantage of fuel-cell based over combustion turbines based power cycles is therefore of about 28-16=12 points; moreover, since almost 50% of energy is directly converted into electricity by the FC, irreversibilities related to thermodynamic processes, that are about 17% in a 55% efficiency combined cycle, will be of about 8 points, for the same thermodynamic quality, thus raising the overall advantage to 12+8=20 points. This means that by proper thermodynamic solutions, combined cycles substituting the combustor with fuel cell can reach efficiencies of about 20 points superior to those of conventional combined cycles based upon gas turbines of "F" technology, i.e. net electrical efficiency in the range of 75%.

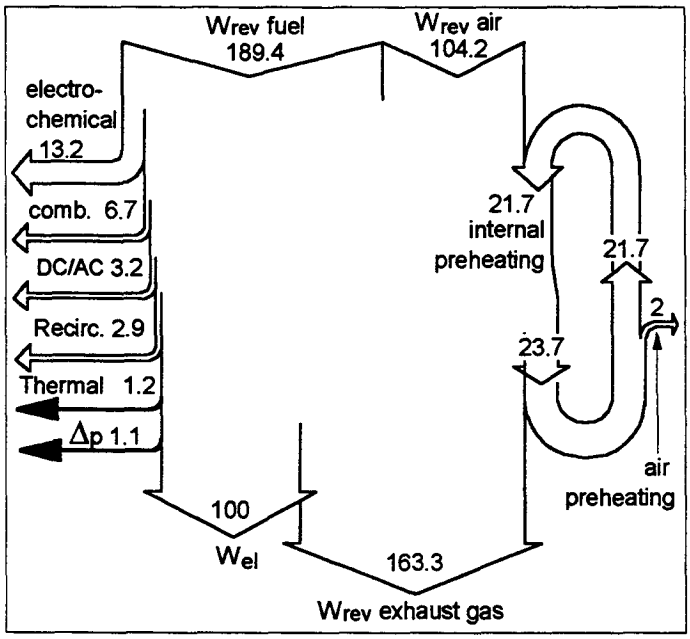

Fig.8: Exergy flows for the pressurized SOFC module of fig. 3.

Coming to the second point, let's consider the Sankey's diagram of fig. 8, representing the reversible work fluxes and second law losses for the SOFC module of fig.3. It can be noticed that the reversible works associated to both exhaust gases and air are larger than the electric energy generated by the cell. It is therefore important to minimize the losses occurring in the thermodynamic path followed to bring ambient air to the pressurized and hot conditions required at fuel cell input, as well as the ones in the processes that return the high temperature pressurized gases exiting the fuel cell to ambient conditions.

3.1 Plant configurations

The three plant configurations shown in fig.9 are investigated:

(A) The scheme is similar to a combined gas/steam cycle, where the combustion process is substituted by the fuel cell. An air preheater is added after the compressor, that recovers heat from gases coming from the fuel cell, before gas turbine expansion; fuel is heated by hot gases up to the temperature required for the desulfurization process.

(B) A recuperative gas turbine cycle is adopted, so that compressed air is heated by low pressure gases after the turbine expansion; a proper bottoming cycle is placed downstream the recuperator.

(C) The arrangement is similar to scheme (B), with the addition of an inter-cooler in the compression phase.

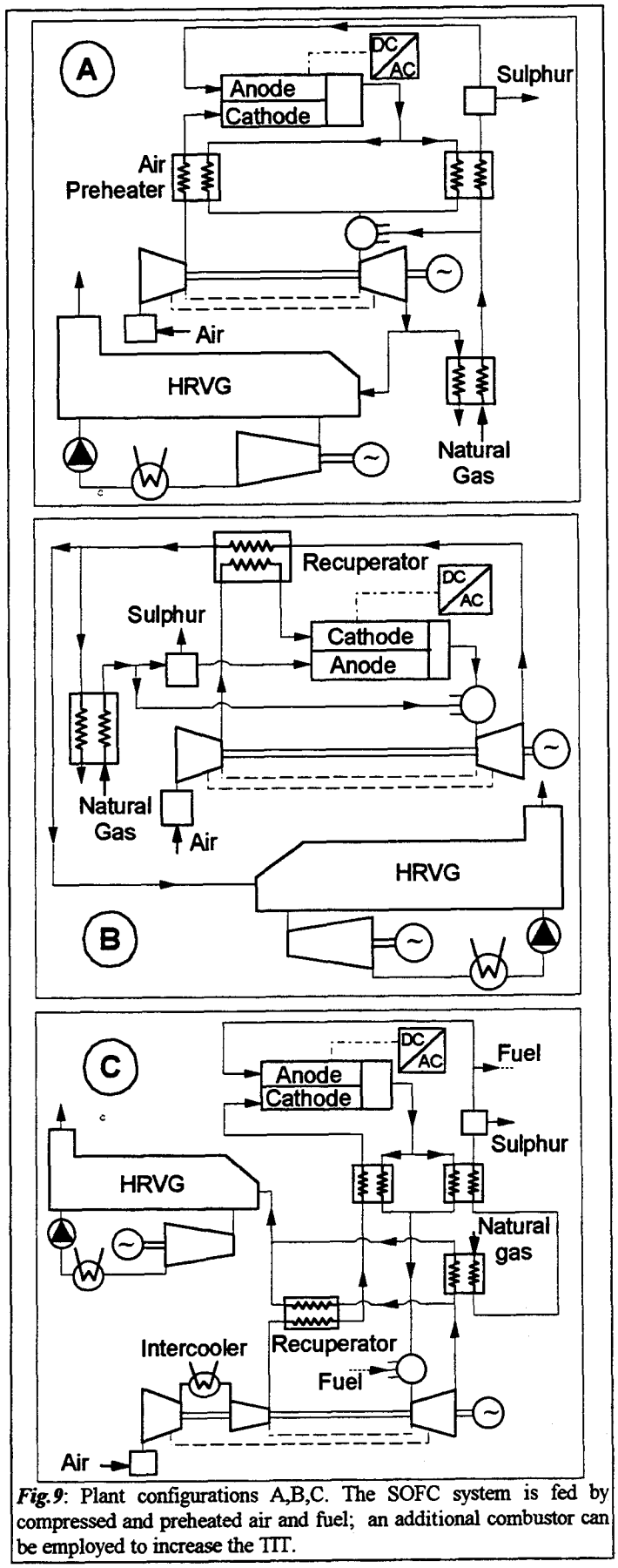

Fig.9: Plant configurations A,B,C. The SOFC system is fed by compressed and preheated air and fuel; an additional combustor can be employed to increase the TIT.

In all three cases, a combustor can be added before the gas turbine to rise the Turbine Inlet Temperature (TIT) to state-of-the art gas turbine technology. As will be discussed later, this addition is detrimental for cycle efficiency, due to the high irreversibilities occurring during combustion and increases NO_x emissions, but has beneficial effects on plant specific costs.Recuperators are kept with $\Delta T_{min} \geq 30°C$ and with wall temperature $\leq 800°C$.

3.2 Results for cycles without combustion

The thermodynamic performance of the three cycles at various pressure ratios are shown in fig. 10: very high net electrical efficiency (lower part of the figure) is obtained by all plant configurations.

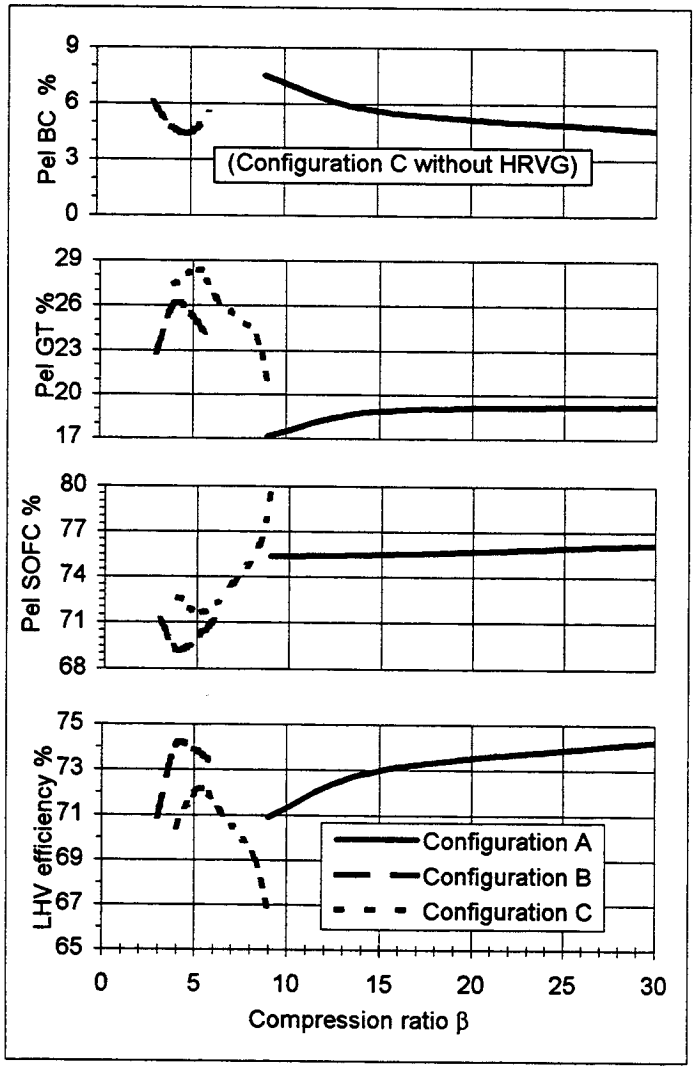

Fig.10: Power distribution and LHV efficiency for configurations A,B,C without firing (mass flow 125 kg/s; BC=bottoming cycle).

A very large portion of the plant electrical output (ranging from 68 and 76%) is generated by the fuel cell; gas turbine contribution is between 18 and 28%, while the output of the bottoming cycle never exceeds 7%. As expected, pressure ratios corresponding to optimum efficiency are low for recuperative cycles (B and C) and high for cycle A. Detailed energy balances and thermodynamic conditions for optimum pressure ratio are given in fig. 12-13-14. For cycle A, a pressure ratio of 30 is assumed (this value is typical for modern aero-derivative units); the gas turbine operates at relatively low temperatures so that the power output is about 40% the one of a conventional unit having the same flow rate and pressure ratio.Owing to low TIT, the turbine blades can be uncooled. The low temperature at gas turbine exit calls for an ammonia, non-recuperative bottoming cycle. Cycle B reaches the same high net electrical efficiency (over 74%) with a pressure ratio close to 5, hence with inherently cheaper turbomachines, but the heat transfer duty of the recuperator is much more demanding than the one of the air preheater of cycle A; gas turbine output is about 30% larger, while gas temperature at heat recovery boiler inlet is as in the first case close to 250 °C. The intercooled, recuperative cycle C reaches an optimum efficiency about 2 points lower than the other two cycles; however, it has the significant advantage of not requiring a bottoming cycle, with obvious savings in plant cost and simplicity.

3.3 Results for cycles with combustion

The addition of a combustor, raising the TIT up to the state-of-the-art value of 1280 °C, remarkably modifies the performance of cycles. Results are summarized in fig. 11.

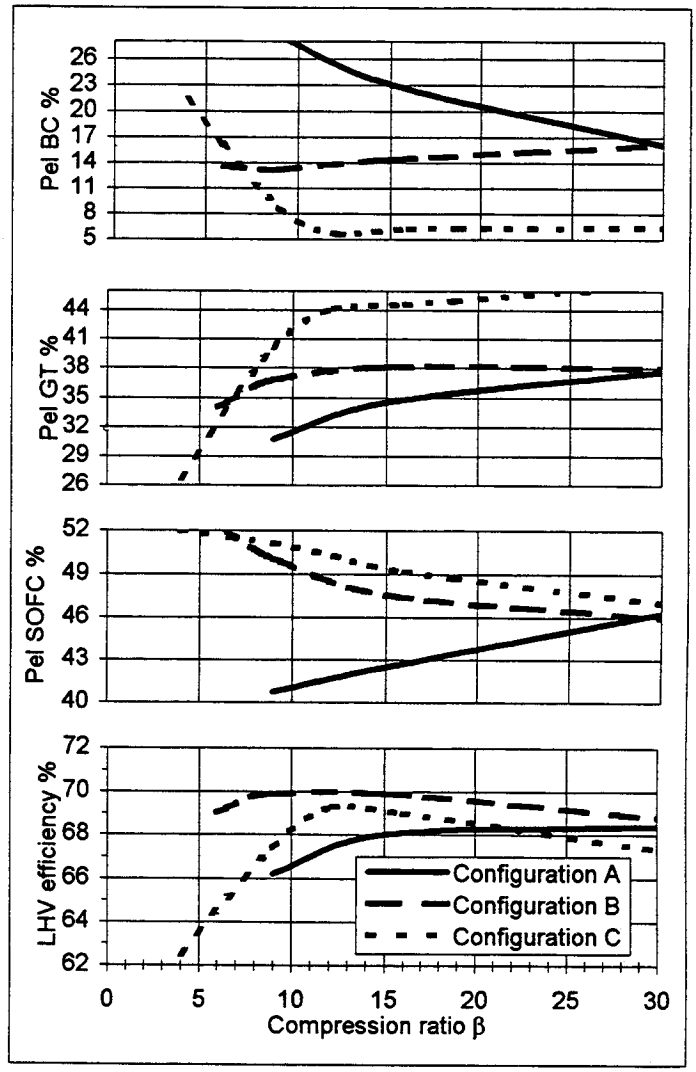

Fig.11: Power distribution and LHV efficiency for configurations A,B,C with TIT=1280°C (mass flow 600 kg/s; BC=Bottoming cycle).

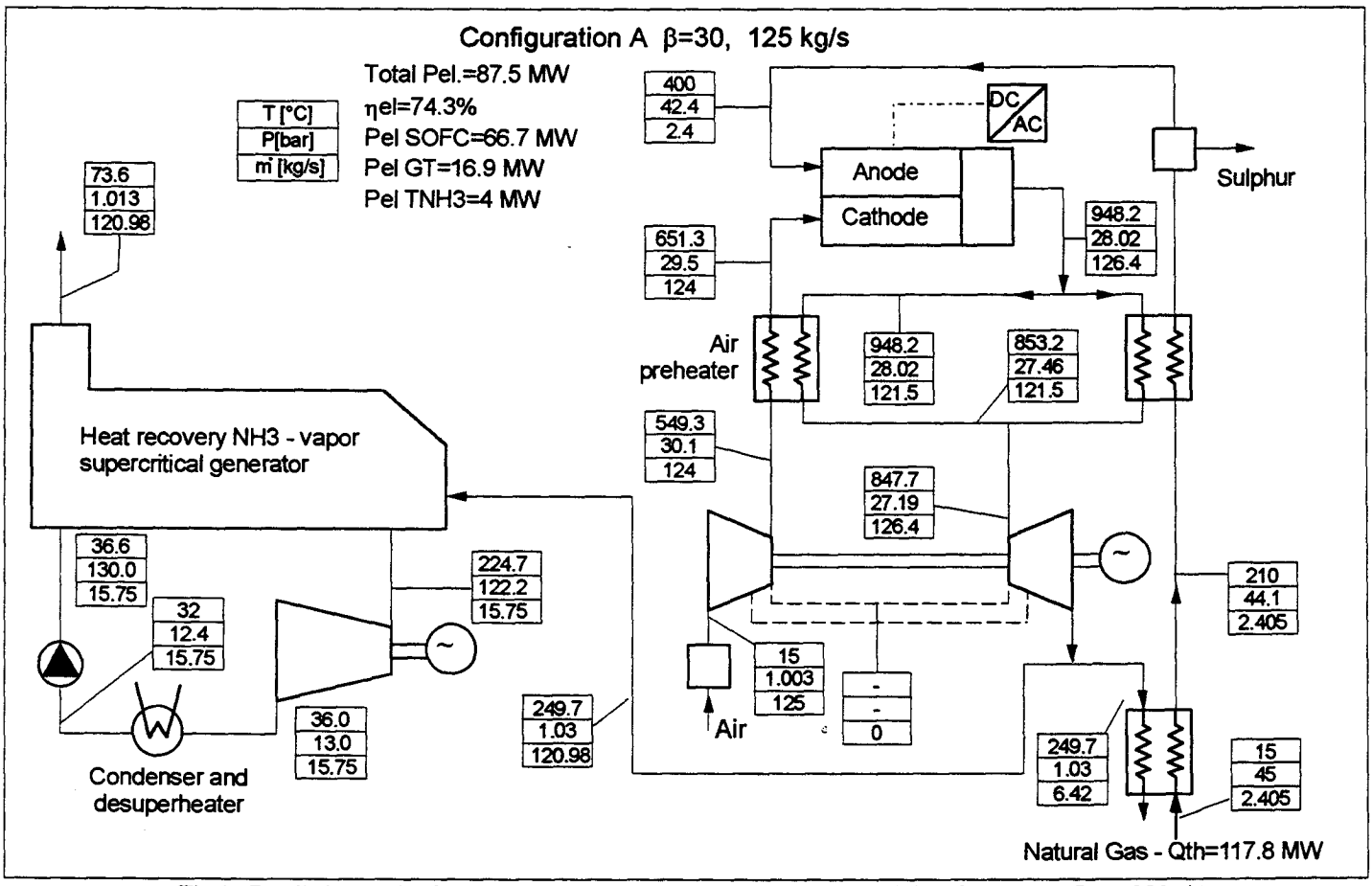

Fig.12: Detailed analysis of configuration A at maximum efficiency without firing (β=30, mass flow 125 kg/s).

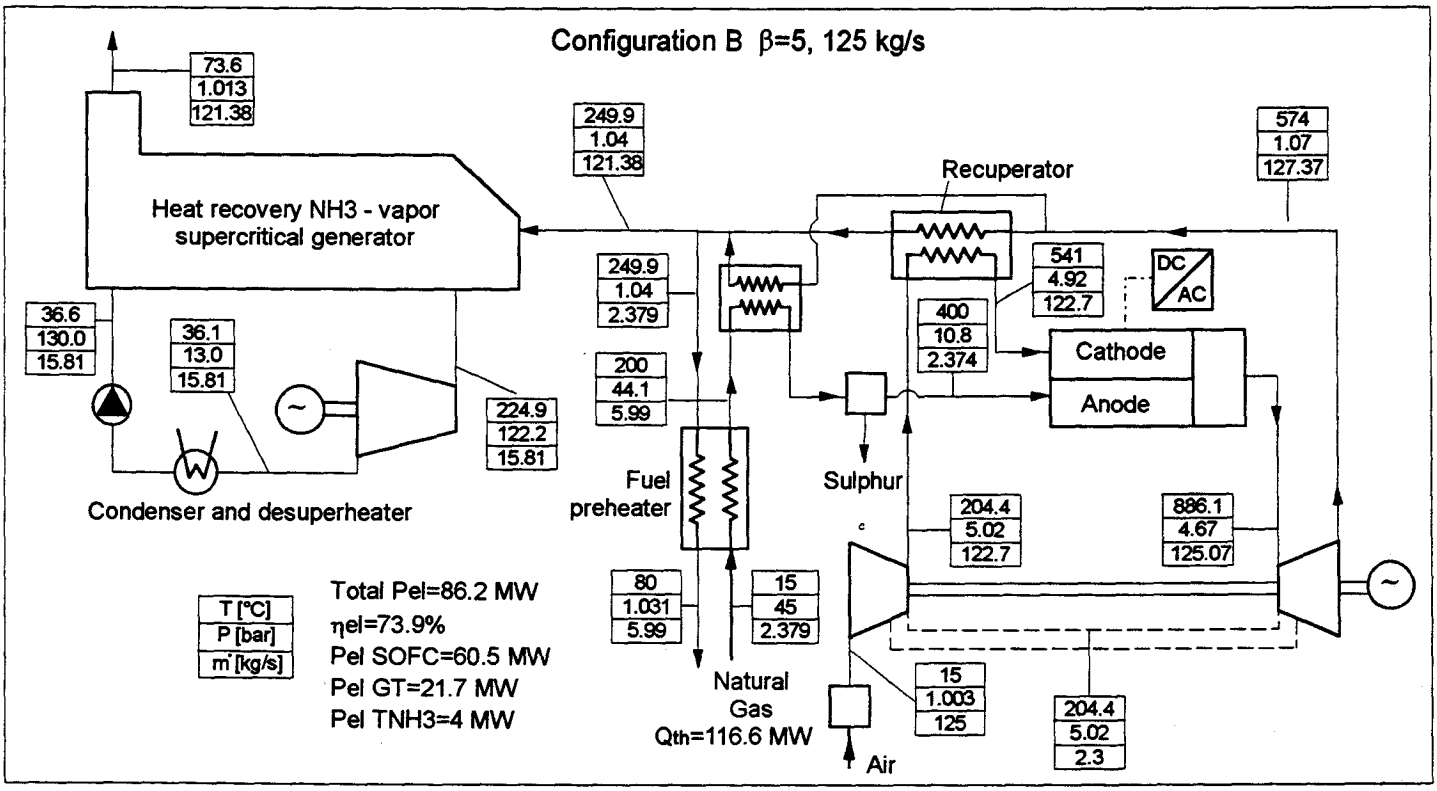

Fig.13: Detailed analysis of configuration B at maximum efficiency without firing (β=5, mass flow 125 kg/s).

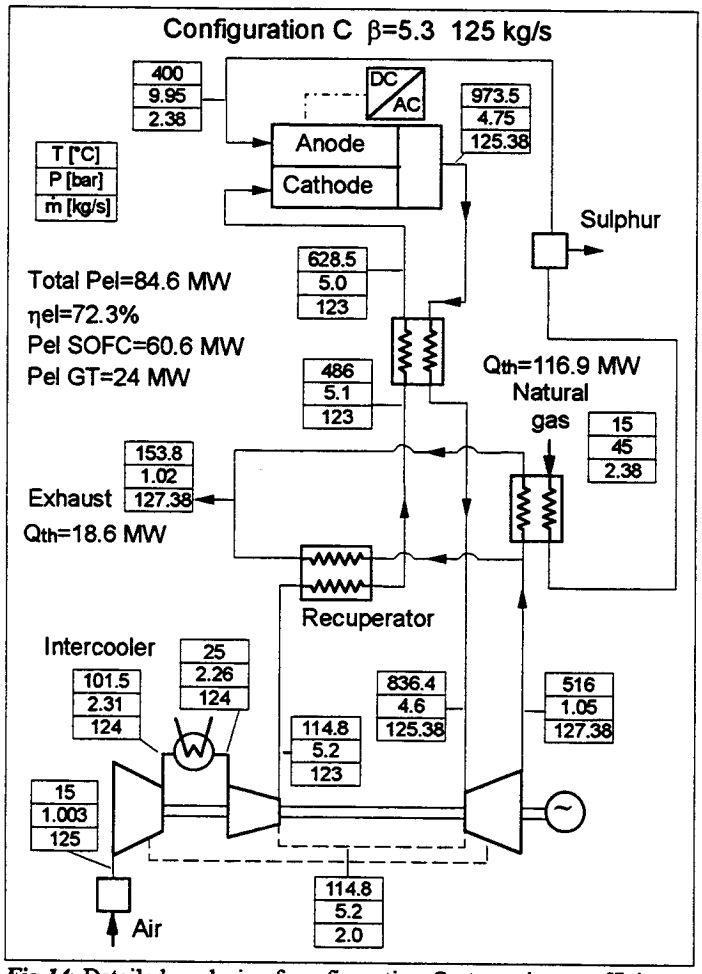

Fig.14: Detailed analysis of configuration C at maximum efficiency without firing (β=5.3, m_a=125 kg/s). No heat recovery bottoming cycle is employed, given the low temperature of exhaust gases.

Maximum values of net electrical efficiency drop to about 70%; the repartition of power production also changes: SOFC share decreases to about 50% of the overall electrical output; the remaining 50% is given by the gas turbine (about 35%) and by the bottoming cycle (about 15%).

Specific works reach values of about 900 kJ/kg, remarkably larger (about 35%) than those of cycles without combustion. The most interesting configuration appears to be cycle B, that reaches the optimum efficiency at pressure ratios close to 15. A detailed energy balance of this situation is shown in fig.15, which refers to an air flow of 600 kg/s, a value representative of the largest gas turbines commercially available in the 50 Hz market. The plant net electrical output is close to 550 MW, about 60% larger than the one of a Natural Gas Combined Cycle (NGCC) built around the same gas turbine. Gas turbine power output is about 7% lower than a conventional machine, due to larger pressure drops in the loop, while steam turbine output is about 60%, due to the presence of the recuperator ahead of the HRSG. Most of the components present in the cycle, including all turbomachines, are either commercially available, or do not present demanding design characteristics, with the only exception of the combustor, that operates at very high (about 900 °C) inlet temperature and relatively low (9%) oxygen content. Similar operating conditions are however technically feasible, as demonstrated by the successful operation of the ABB reheat turbine (Jury and Luthi, 1994).

Configuration A appears to be somewhat less attractive: it reaches lower (about 2%) efficiency and specific work, and requires higher pressure ratios and therefore more costly turbomachines. These effects are probably not counterbalanced by the less demanding heat transfer equipment (the air preheater instead of the recuperator). Also the addition of an intercooling (configuration C) does not appear to be advantageous: the efficiency and the specific work do not increase, while the thermal duty of the recuperator is remarkably larger.

3.4 Second-law Analysis

A better thermodynamic understanding of the above described results can be obtained by means of the second law analysis. Table 2 gives the various second-law efficiency losses, grouped in the following nine terms:

- irreversibilities occurring in the fuel cell (including power conditioning, heat exchange, combustion, heat losses, pressure drops, etc.)
- irreversibilities occurring in the combustor ahead of the gas turbine (when present)
- fluid-dynamic losses during air compression
- fluid-dynamic losses during gas expansion, including losses related to blade cooling (when present)
- heat transfer, heat losses and pressure drops (both side) occurring in the recuperator or air preheater
- heat transfer, heat losses and pressure drops occurring in all other heat exchangers (in the air/gas loops), including fuel preheaters
- all mechanical, electrical, auxiliary losses related to the air/gas loops
- all irreversibilities occurring in the bottoming cycle
- stack losses.

Five cases are considered (see table 3 for global performance): the three configurations A, B and C without combustion at optimum pressure ratio (fig. 12-13-14), the configuration B with combustion (fig. 15) and, as a reference, a combined cycle based upon the same technological assumptions (NGCC). The following general comments can be made in comparing the three cycles without combustor to conventional combined cycle:

- SOFC losses are about 11-13 lower than the combustion losses occurring in NGCC
- losses related to bottoming cycle are much lower, owing to the much lower temperature of gases entering the HRVG
- gas turbine losses are also much lower, mainly because of the absence of cooling flows
- stack losses are also lower, due to the low temperature of exhaust gases
- losses related to recuperator (or air preheater) are relatively small.

With reference for example to cycle B, the efficiency gain of about 20 points is therefore given not only by the more reversible oxidation process adopted (about 11 points), but also by lower bottoming cycle losses (over 5 points), lower gas turbine losses (2.9 points), lower stack losses (0.6 points), lower compressor losses (0.8 points), etc.

Configuration A reaches an efficiency similar to that of case B, but with a different loss distribution: the SOFC losses are lower, since the cell operates at higher pressure and temperatures, but this gain is counterbalanced by the larger losses required for compressing air at much higher pressures. The intercooling (cycle C) yields positive

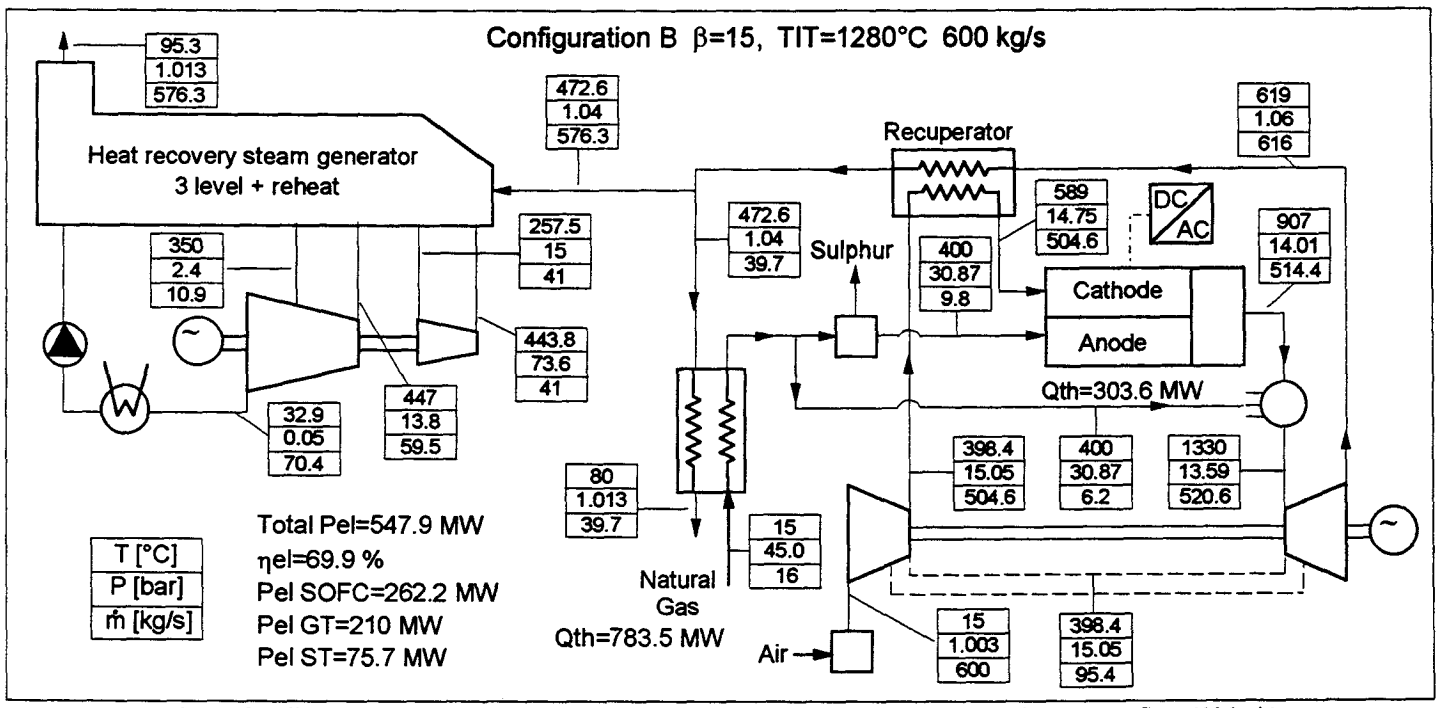

Fig.15: Detailed analysis of configuration B at maximum efficiency with TIT=1280°C (β=15, mass flow 600 kg/s).

II Principle efficiency loss.	Cycle A β=30 nc	Cycle B β=5 nc	Cycle C β=5.3 nc	Cycle B β=15 TIT 1280°C	NGCC β=15 TIT 1280°C
SOFC	15.48	17.81	16.84	10.66	-
Combustor GT	0	0	0	8.608	28.8
Compressor	3.42	1.63	1.55	1.923	2.43
Gas Turbine	2.13	2.01	1.35	3.464	4.95
Recuperator ($\Delta T,\Delta p,\eta_{th}$)	1.43	1.48	1.85	0.574	-
Other heat exchangers ($\Delta T,\Delta p,\eta_{th}$, mix)	0.86	0.97	3.95	0.486	-
Aux, mec., org., electric GT and compressor losses	0.705	0.535	0.61	0.595	0.69
Bottoming cycle (including aux)	3.1	3.08	0	4.52	8.48
Stack (exhaust gas)	0.775	0.755	3.85	1.45	1.38
Wel total (η_{II})	72.1	71.73	70	67.67	53.27
Wel/LHV (η_{el})	74.7%	74.2%	72.3%	70%	55%

Tab.3: Entropy analysis for selected configurations and for a proven-technology combined cycle (NGCC).

	Cycle A β=30 nc	Cycle B β=5 nc	Cycle C β=5.3 nc	Cycle B β=15 TIT 1280°C	NGCC β=15 TIT 1280°C
Air flow at filter inlet (kg/s)	125	125	125	600	600
Combustor-FC outlet temperature / TIT (°C)	848/848	888/883	836/836	1330/1280	1336/1280
SOFC system power (MW)	66.6	60.5	60.6	262.2	-
GT power (MW)	16.9	21.7	24	210	214.6
Power SOFC+TG (MW)	83.5	82.2	84.6	472.2	-
T exhaust (HRVG inlet) (°C)	249.7	249.9	156	472.6	596
Bottoming cycle power (steam/ NH_3) (MW)	- / 4.0	- / 4.0	-/-	75.7 / -	123.1/-
Power SOFC+TG +bottoming cycle (MW)	87.5	86.2	84.6	547.9	337.7
η_{el} without bottoming cycle	70.9%	70.4%	72.3%	60.3%	35%
η_{el} with bottoming cycle	74.3%	73.9%	-	69.9%	55%
Reversible power exhaust gas (MW)	8.8	8.9	4.1	123	180
Thermal power exhaust gas (cooled at 25°C) (MW)	30	30	18.6	290	392
Thermal power exhaust gas (cooled at 70°C) (MW)	24	24	12	258	360
I law efficiency with cogeneration (T stack = 70°C)	91.2%	91%	83%	93%	93%

Tab.4: Global performances for selected configurations and for a proven-technology combined cycle (NGCC).

effects on FC and turbomachines losses, but introduces significant penalties in the intercooling process; moreover, the absence of the bottoming cycle increases stack losses.

4. ECONOMIC ANALYSIS

Both simple cycle (configuration A) and recuperated cycle (configuration B) yield efficiency close to 75%: in the first case higher pressure ratio and consequently more complex and costly turbomachines are required, while in the latter the heat exchanger duty becomes more relevant. Intercooling does not give advantages in efficiency, but allows simpler plant configuration, by avoiding the bottoming cycle. The key factor in selecting one of the two schemes will probably be the influence of the operating pressure on fuel cell system cost and life. The economic outlook of these solutions is strictly related to the specific investment cost and operating life of SOFC; moreover, the specific cost of the "conventional" part of plant, i.e. gas turbine and bottoming cycle will also be significant, since large air quantities are to be handled in relation to the added power output. These solutions are particularly promising for medium-size cogeneration applications, where higher specific capital costs can be accepted.

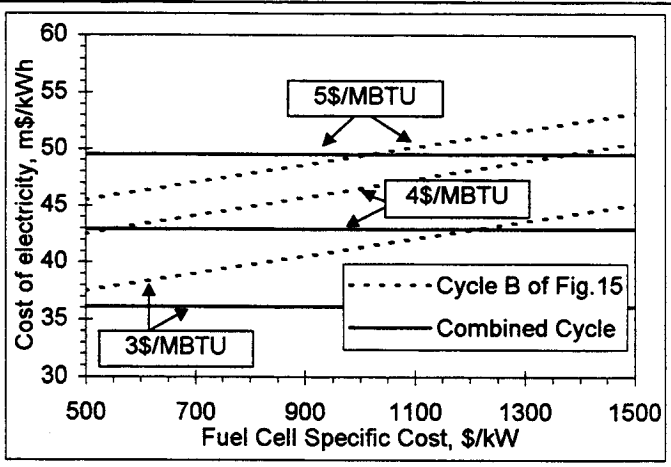

Fig.16: Cost of electricity for a proven-technlogy combined cycle and for the power cycle of fig. 15 (β=15, TIT=1280°C); three different scenarios are considered, with the natural gas cost ranging from 3 $/MBTU to 5 $/MBTU and with SOFC system cost of 500÷1500 $/kW. The following assumptions are made: (i) investment costs annualized with a 12% interest rate and 15% years plant life; (ii) for NGCC, investment cost, including interest during construction is 605 $/kW; (iii) O&M cost is 6 mills/kWh, (iv) net electrical efficiency is 55%, (v) the annual electricity generated is 7900 kWh/kW. For plant of fig.13: (i) the specific cost of "conventional equipment" is assumed equal to 400 $/kW of global output of turbogenerators, (ii) 305 $/kW are added for accounting for general facilities, project and process contingencies, interest during construction, etc; (iii) O&M specific costs are assumed equal 9 mills/kWh. The specific cost of SOFC accounts for all repair and substitution costs during the stipulate 15 years plant life.

The addition of a combustor that raises the TIT to the values adopted by modern state-of-the art gas turbines penalizes the efficiency of about 5 points. However, the efficiency is still extremely high (close to 70%) and benefits related to ambient (Low NO_x, low CO_2 emissions) are still relevant. The advantage brought about by combustion is that, compared to SOFC-alone electrical power, the global plant electrical output is more than doubled: as a consequence, since the SOFC is the most costly component, the overall specific cost will decrease.

Referring to the example of fig. 15, all plant components but SOFC are conventional and their cost can be precisely estimated. It is therefore possible to predict the influence of SOFC specific cost on cost of electricity for a large-scale, base-load power plant.The results of this calculation are shown in fig. 16. It is shown that the SOFC based cycle, in spite of its better efficiency, cannot economically compete with conventional combined cycle for natural gas prices below 4 $/MBTU: the breaking point can be reached only by the following contemporary occurrence: cost of natural gas higher than present values (5 $/MBTU) and a SOFC cost of 1000 $/kW, a value sometimes quoted in the literature (Stephenson and Ritchey, 1997; Killerud et al., 1997).

5. CONCLUSIONS

The thermodynamic advantages achievable by substituting the combustion process occurring in a conventional combined cycle with a SOFC are conspicuous: the net efficiency raises of about 20 points, i.e. efficiencies close to 75% can be reached with present gas turbine technology both with simple cycle (configuration A) and recuperated cycle (configuration B).

With respect to conventional combined cycles:

- larger air flows are to be handled in relation to the added power output (reaching 700÷900 kJ/kg);
- efficiencywise, it is better to avoid additional combustion process outside the fuel cell: this yields unusually low gas turbine operating temperatures;
- intercooling allows simpler plant configuration, by avoiding the bottoming cycle without efficiency penalties;
- higher specific capital costs and higher cost of electricity for natural gas prices below 4 $/MBTU are foreseeable.

References

Achenbach E. (1994) "Three-dimensional and time-dependent simulation of a planar solid oxide fuel cell stack", Third Grove Fuel Cell Symposium, UK, 1993; J.of Power Sources 49 (333-348), 1994.

Ahmed S., McPheeters C., Kumar R. (1991) "Thermal-hydraulic model of a monolithic solid oxide fuel cell", J.of the Electrochem. Soc.,vol.138, n.9,1991.

Appelby A.J., Foulkes F.R. (1989) "Fuel cell handbook", Van Nostrand-Reynolds,1989

Appelby A.J. (1994), "Fuel cell electrolytes:evolution, properties and future prospects", Third Grove Fuel Cell Symposium, UK,1993: Journal of Power Sources, 49(15-34), 1994.

Appelby A.J. (1995) "Fuel cell technology: status and future prospects", Energy-The international Journal, 1995

Bessette N.F., George R.A.(1996) "Electrical performance of Westinghouse's AES solid oxide fuel cell", 2nd Int.nal Fuel Cell Conference, (IFCC 4-12) Japan, 1996

Bevc F.P., Lundberg W.L., Bachovchin D.M. (1996) "Solid Oxide Fuel Cell combined cycles", ASME 96-GT-447 June 1996.

Campanari S., Lozza G., Macchi E. (1995) "Comparative thermodynamic analysis of ammonia, air and steam cycles for heat recovery from gaseous flows" (in Italian), VIII congress Technologies and Complex Energetic Systems "Sergio Stecco", Bologna, Italy, June 1995.

Campanari S., Macchi E. (1997) "Integrated cycles with solid oxide

fuel cells and gas-steam combined cycles" (in Italian), IX congress Technologies and Complex Energetic Systems"Sergio Stecco", Milano, Italy, June 1997.

Chiesa P.,Consonni S., Lozza G. and Macchi E. (1993) "Predicting the ultimate performance of advanced power cycles based on very high temperature gas turbine engines", ASME paper 93-GT-223, 1993

Consonni S., Lozza G., Macchi E., Chiesa P., Bombarda P. (1991) "Gas-Turbine-Based Advanced Cycles for Power Generation Part A: Calculation Model" Int.nal Gas Turbine Conference-Yokohama 1991, Vol III pp. 201-210, 1991.

Consonni S. (1992) "Performance prediction of gas/steam cycles for power generation", MAE Dept. Ph.D. Thesis n.1893-T, Princeton University, Princeton, NJ.

Consonni S., Macchi E. (1996) "Externally fired combined cycles. Part A:Thermodynamics and technological issues / Part B:Alternative configurations and cost projections", ASME papers 96-GT-92 and 96-GT-93.

Hirschenhofer J.H., Stauffer D.B., Engleman R.R. (1994) "Fuel cells, a handbook (Rev.3)", Gilbert/ Commonwealth Inc. for U.S. Department of Energy (DOE), 1994

Hirschenhofer J.H. (1996) "1996 Fuel cell status", proc. of the 31st IECEC, no.96353, p.1084-1092.

Hsu M., Nathanson D., Hoag E. (1994) "ZTEK advanced planar SOFC for atmospheric and pressurized operation", Proc. of the 29th IECEC, vol.2, 1994.

Ide H. et al. (1989), "Natural gas reformed fuel cell power generation systems - A comparison of three system efficiencies" Proc.of the 24th IECEC, Washington, 1989.

Itoh H., Mori M., Mori N., Abe T. (1994) "Production cost estimation of solid oxide fuel cells" Journal of Power Sources, 49 (1994) 315-332, 1994.

Juri W.,Luthi H.K. (1994) "Advanced GT's call for advanced CC's" ASME 94-GT-303, The Hague, June 1994.

Kaneko S., Gengo T., Uchida S. e Yamauchi Y. (1991) (Mitsubishi H.I. Ltd) "Research and development of Solid Oxide Fuel Cells" SOFC Symposium 1991.

Kinoshita K., McLarnon F.R., Cairns E.J. (1988), "Fuel cells, a handbook", L.Berkeley Laboratory for U.S. DOE, 1988.

Killerud K., Ødegård R., Kløv K. (1997), "FP-O2: Perspectives of solid oxide fuel cells in the natural gas industry" IGU- 20th World Gas Conference Proceedings, Copenaghen, 1997.

Lobachyov K., Richter H.J. (1996), "Combined cycle gas turbine power plant with coal gasification and Solid Oxide Fuel Cell" Journal of Energy Resources technology, Vol.118, Dec.1996.

Lobachyov K., Richter H.J. (1997),"Addition of highly efficient bottoming cycles for the nth-generation molten carbonate fuel cell power plant", Journal of Energy Resources technology, Vol.119, June 1997.

Lundberg W.L. (1990) "System applications of tubular solid oxide fuel cells" proc. of the 25th IECEC pp.218-223, 1990 .

Lozza G. (1990)"Bottoming steam cycles for combined gas-steam power plants: a theoretical estimation of steam turbine performance and cycle analysis" , proc. 4th ASME Cogen Turbo, New Orleans, Louisiana (USA), pp.83-92, 1990.

Lozza G. (1993) "Steam cycles for large-size-high-gas-temperature combined cycles", proc. of the 7th ASME Cogen Turbo Power, Bournemouth, UK, pp.435-444, 1993.

Lozza G., Chiesa P., DeVita L. (1996) "Combined-cycle power stations using Clean-coal technologies: thermodynamic analysis of full gasification vs fluidized bed combustion with partial gasification", Journal of Engineering for Gas Turbine and Power, Vol. 118, n.4, Oct.1996.

Macchi E., Perdichizzi A. (1981) "Efficiency prediction for axial-flow turbines operating with non-conventional fluids", Journal of Engineering for Power, Vol.103, pp.718-724, October 1981.

Macchi E. et al. (1994) "An assessment of the thermodynamic performance of mixed gas-steam cycles. Part A: Intercooled and steam-injected cycles / Part B: Water-injected and HAT cycles", ASME 94-GT-423 and 94-GT-424, 1994.

Mozzafarian M. (1994) "Solid oxide fuel cell for combined heat and power applications" Proc. of the First European Solid Oxide Fuel Cell Forum, Lucerne, Switzerland 1994

Penner S.S., Appelby A.J. et al. (1995) "Commercialization of Fuel Cells" Energy, The International Journal, Vol.20, No.5, pp.331-470, 1995

Ray E.R., Ruby J.D.(1992) "Evaluation of the Westinghouse Solid Oxide Fuel Cell technology for electric utility applications in Japan" EPRI TR-100713,1992

Stephenson D., Ritchey I. (1997) "Parametric study of fuel cell and gas turbine combined cycle performance", ASME 97-GT-340.

Veyo S. (1996 a) "The Westinghouse SOFC program - a status report", proc. 31st IECEC, paper n.96570, p.1138, 1996.

Veyo S. (1996 b) "Westinghouse fuel cell combined cycles", Federal Energy Technology Center FC Conference, Morgantown, Aug.1996.